Structural Engineering and Mechanics, Vol. 33, No. 6 (2009) 657-674
DOI: http://dx.doi.org/10.12989/sem.2009.33.6.657

Failure analysis of laminates by implementation of continuum damage mechanics in layer-wise finite element theory

B. Mohammadi†

School of Mechanical Engineering, Iran University of Science and Technology, University Road, Hengam Street, Resalat Square, Narmak, Tehran, Iran

H. Hosseini-Toudeshky‡

Aerospace Engineering Department & Center of Excellence in Computational Aerospace Engineering, Amirkabir University of Technology, No. 424, Hafez Ave., Tehran, Iran

M.H. Sadr-Lahidjani‡†

Aerospace Engineering Department, Amirkabir University of Technology, No. 424, Hafez Ave., Tehran, Iran

(Received November 22, 2007, Accepted September 25, 2009)

Abstract. In this paper a 3-D continuum damage mechanics formulation for composite laminates and its implementation into a finite element model that is based on the layer-wise laminate plate theory are described. In the damage formulation, each composite ply is treated as a homogeneous orthotropic material exhibiting orthotropic damage in the form of distributed microscopic cracks that are normal to the three principal material directions. The progressive damage of different angle ply composite laminates under quasi-static loading that exhibit the free edge effects are investigated. The effects of various numerical modeling parameters on the progressive damage response are investigated. It will be shown that the dominant damage mechanism in the lay-ups of [+30/-30]s and [+45/-45]s is matrix cracking. However, the lay-up of [+15/-15] may be delaminated in the vicinity of the edges and at $+\theta/-\theta$ layers interfaces.

Keywords: continuum damage mechanic; angle ply laminate; layer-wise; FEM.

1. Introduction

The analysis of composite structures may require the construction of damage models capable of predicting the different damage mechanisms and their evolution until final fracture. In addition,

† Assistant Professor, E-mail: Bijan_Mohammadi@iust.ac.ir
‡ Associated Professor, Corresponding author, E-mail: Hosseini@aut.ac.ir
‡† Assistant Professor, E-mail: Sadr@aut.ac.ir

these models should be applicable to industrial structures subjected to complex loading.

An attractive framework for derivation of material models considering local failure is continuum damage mechanics (CDM). In this concept, the local loss of load-carrying area due to formation of microcracks is accounted for by damage internal variables. Kachanov (1958), Lemaitre (1985 and 1986), Chaboche (1988a and 1988b) and Krajcinovic (1983 and 1984) used continuum damage mechanics to analyze different types of damage ranging from brittle fracture to ductile failure. However, the application of continuum damage mechanics to composite materials has been restricted for composites utilizing a transversely isotropic medium (Talreja 1985).

Ladeveze *et al.* (1990) developed a *meso* scale shell model for laminated composites. Ladeveze and Le Dantec (1992), Allix and Ladeveze (1989 and 1992) and Ladeveze *et al.* (2000) continued with the mesomechanical modeling where damage was independently predicted for each homogenized composite ply, and each interface that separates adjacent plies. The laminate was assumed to break into a series of anisotropic plies, which are homogeneous through the thickness, and zero-thickness interface layers. By analyzing each ply at the fiber, matrix, and fiber/matrix interface levels, qualitative information were provided about the fiber and matrix properties of the laminate (Ladeveze 1990). Damage was also based on two independent modes; one representing matrix cracking and fiber pull-out while the second was associated with the transverse brittle failure of the fiber-matrix interface. The interface model incorporates three damage parameters, each associated with a through-thickness stress, one normal, and two shears.

Voyiadjis and Kattan (1993 and 1999), Voyiadjis and Park (1999) and Voyiadjis and Deliktas (2000) developed a 3-D model for coupled progressive damage and plasticity using a symmetric second order damage tensor. Voyiadjis and Park (1993) and Voyiadjis and Deliktas (2000) proposed a micromechanical based approach that incorporated damage and plastic deformations into the analysis of metal matrix composite materials. They characterized three damage modes: matrix damage, fiber damage, and interfacial debonding. An isotropic damage criterion was also proposed for the three types of damages accompanied by damage evolution equations assuming that the energy dissipated due to the plasticity and that due to the damage were independent of each other.

Barbero and De Vivo (2001) developed a 2-D plane stress model for progressive damage based on the use of a symmetric second order damage tensor. Damage evolution and stiffness reduction were computed for the pre-homogenized composite material simplifying the formulation. Their model was extended by Barbero and Lonetti (2002) to include plasticity, and further extended by Lonetti *et al*. (2003) to include triaxial orthotropic damage in terms of three damage eigenvalues.

Two-dimensional damage models are usually employed when plane stress or strain conditions are imposed. Obviously, these conditions are not fulfilled for the analysis of real structures. For such structures, the three-dimensional modeling becomes necessary. However, the use of three-dimensional models is limited to the prediction of the elastic properties and/or the initial damage, and not for the distinction of other important damage aspects such as the damage modes.

In this paper, progressive damage of the composite laminates under quasi-static, monotonic loading are investigated. For this purpose continuum damage mechanics incorporated with a special layer-wise laminated plate theory is used. The purposed CDM model uses the hypothesis of strain energy equivalency to relate the damage and fictitious undamaged state; however in the Ladeveze approach the strain equivalency was used. In the present method we also used the associated flow rule, but Ladeveze used the lay-up dependent non-associated flow rule. In our approach, the eigenvalues of the damage tensor is capable of quantitatively and indirectly describing the density and distribution of the fiber degradation, fiber/matrix debonding, and matrix cracks that are oriented either parallel to the fibers direction or perpendicular to that. But, Ladeveze didn't use a damage tensor and he implemented the related damage parameters to each damage mode in to the material stiffness matrix directly.

The developed finite element program is displacement based using eight-node 2D elements including special layer-wise laminated plate theory. This layer-wise model uses a reduced constitutive matrix that is based on the assumption of zero transverse normal stress; and also includes discrete transverse shear stresses via in-plane displacement components that are C^0 continuous with respect to the thickness direction. The 3D CDM model is summarized for the special case of orthotropic damage, culminating in the damaged constitutive relations and the governing equations that drive the evolution of the internal damage variable. Details of the numerical implementation of the 3-D CDM model into the layer-wise finite element model are also expanded. The numerical examples include laminate problems with angle-ply tensile test specimens that exhibit the free edge effects. The effects of various numerical modeling parameters on the progressive damage response of the laminates are also investigated.

1.1 Constitutive relation for composite lamina with damage

In the CDM, damage variables can be presented through the internal state variables of thermodynamics for irreversible processes in order to describe the effects of damage and its microscopic growth on the macromechanical properties of the materials. Using CDM, distributed microscopic damage can be quantified by the use of a damage tensor field that describes the orientation and density of microcracks in the material. Since CDM involves irreversible phenomena, attention must be paid to restrictions imposed by the first and second principles of thermodynamics.

In a homogenized description, the simplest form of the damage tensor that is capable of accurately describing microscopic damage is a symmetric 2nd order tensor $\boldsymbol{\varphi}$ whose principal directions are assumed to coincide with the principal material directions (Barbero 2001), i.e., orthotropic damage. In this case, the eigenvalues of $\boldsymbol{\varphi}$ (denoted φ_1, φ_2, and φ_3) have a simple physical interpretation. The ith eigenvalue φ_i represents the effective fractional reduction in load carrying area on planes that are perpendicular to the ith principal material direction. Therefore, this type of damage tensor field is capable of quantitatively describing the density and distribution of microscopic cracks that are associated with fiber breakage, fiber/matrix debonding, and matrix cracks that are oriented either parallel to the fibers direction or perpendicular to that as shown in Fig. 1. The eigenvalues of the damage tensor are in the range $0 < \varphi_i < 1$ where $\varphi_i = 0$ corresponds to a complete lack of damages normal to the ith principal material direction, while $\varphi_i = 1$

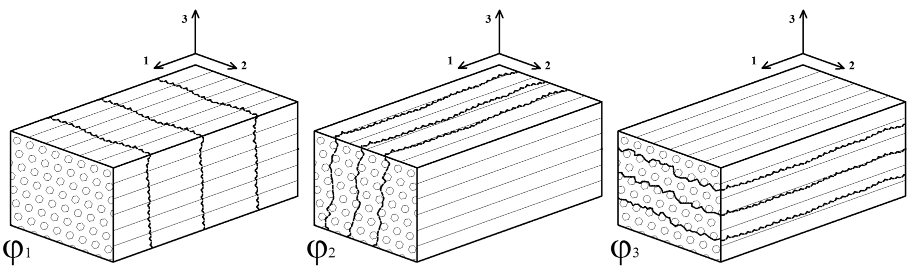

Fig. 1 Distribution of microcracks described by damage eigenvalues φ_1, φ_2 and φ_3 normal to the ith principal material direction

corresponds to a complete separation of the material across the planes normal to the ith principal material direction.

1.2 Stress transformation and stiffness definition

In a general state of deformation and damage, the effective stress tensor in fictitious undamaged state, $\bar{\boldsymbol{\sigma}}$, is related to the Cauchy stress tensor in damage state, $\boldsymbol{\sigma}$, by the following linear transformation (Kachanov 1958)

$$\bar{\boldsymbol{\sigma}} = M(\boldsymbol{\varphi}):\boldsymbol{\sigma} \tag{1}$$

where **M** is a fourth-order linear transformation operator called the damage effect tensor. Depending on the form used for **M**, it is very clear from Eq. (1) that the effective stress tensor $\bar{\sigma}$ is generally non-symmetric. However, the use of such complicated mechanics can be easily avoided by symmetrizing the effective stress. One of the symmetrization methods given by Cordebois and Sidorof (1979) is used in this study, and is expressed as follows

$$\bar{\sigma}_{ij} = (\delta_{ik} - \varphi_{ik})^{-1/2}\sigma_{kl}(\delta_{jl} - \varphi_{jl})^{-1/2} \tag{2}$$

where $\boldsymbol{\delta}$ is the Kronecker delta, and $\boldsymbol{\varphi}$ is second-order damage tensor. Corresponding to Eq. (2), the fourth-order damage effect tensor, **M**, is

$$M_{ikjl} = (\delta_{ik} - \varphi_{ik})^{-1/2}(\delta_{jl} - \varphi_{jl})^{-1/2} \tag{3}$$

It is possible to define Hooke's law in the effective fictitious undamaged and damaged state as follows

$$\bar{\boldsymbol{\sigma}} = \bar{\mathbf{C}}^e:\bar{\boldsymbol{\varepsilon}}^e; \qquad \boldsymbol{\sigma} = \mathbf{C}^e(\boldsymbol{\varphi}):\boldsymbol{\varepsilon}^e \tag{4}$$

where an over-bar indicates that the quantity is evaluated in the effective configuration and the superscript e denotes quantities. Damaged material stiffness at each step can be expressed in terms of the damage eigenvalues by invoking various strain energy equivalence principles, which states that the elastic energy of the damaged material is in the same form as that of the effective material, which the stress tensor is replaced by the effective stress (Voyiadjis 2000).

$$\mathbf{C}^e(\boldsymbol{\varphi}) = \mathbf{M}^{-1}:\bar{\mathbf{C}}^e:\mathbf{M}^{-1} \tag{5}$$

In Eq. (5), $\bar{\mathbf{C}}^e$ and $\mathbf{C}^e(\boldsymbol{\varphi})$ are virgin material stiffness, and damaged stiffness matrix of material respectively.

1.3 State laws in the framework of irreversible thermodynamics

Since the internal state variables are selected independently, it is possible to decouple the Helmholtz free energy, ψ, into a potential function for each corresponding internal-state variable. Therefore, an analytical expression for the thermodynamic potential can be given as the summation of the two terms of, strain energy, $E(\boldsymbol{\varepsilon}^e, \boldsymbol{\varphi})$, and dissipation energy, $\Pi^d(\kappa)$, as follows (Voyiadjis 2000)

$$\rho\psi = E(\boldsymbol{\varepsilon}^e, \boldsymbol{\varphi}) + \Pi^d(\kappa) \tag{6}$$

where κ is the internal variable indicating overall damage. The strain energy is defined (Voyiadjis 2007)

$$E(\boldsymbol{\varepsilon}^e, \boldsymbol{\varphi}) = \frac{1}{2}\boldsymbol{\varepsilon}^{eT}:\mathbf{C}^e(\boldsymbol{\varphi}):\boldsymbol{\varepsilon}^e \tag{7}$$

In addition, the free energy $\Pi^d(\kappa)$ introduced to describe the effect of the accumulated damage can be expressed as follows (Barbero 2002, Voyiadjis 2007)

$$\Pi^d(\kappa) = c_1^d[c_2^d \exp(\kappa/c_2^d) - \kappa]; \quad \text{or} \quad \Pi^d(\kappa) = \frac{1}{2}c_1^d\kappa^2 \tag{8}$$

where c_1^d and c_2^d are the material constants. The state laws can be written from the thermodynamic potential Eq. (6) in the following form (Voyiadjis 2007)

$$\boldsymbol{\sigma} = \rho\frac{\partial\psi}{\partial\boldsymbol{\varepsilon}^e} = \mathbf{C}^e(\boldsymbol{\varphi}):\boldsymbol{\varepsilon}^e \tag{9}$$

$$\mathbf{Y} = -\frac{\partial\psi}{\partial\boldsymbol{\varphi}} = -\frac{1}{2}\boldsymbol{\varepsilon}^{eT}\frac{\partial\mathbf{C}^e(\boldsymbol{\varphi})}{\partial\boldsymbol{\varphi}}\boldsymbol{\varepsilon}^e \tag{10}$$

$$K = -\frac{\partial\psi}{\partial\kappa} = -c_1^d[1 - \exp(\kappa/c_2^d)] \quad \text{or} \quad K = c_1^d\kappa \tag{11}$$

where $\boldsymbol{\sigma}$, $\mathbf{Y}$, and K are stress tensor, damage conjugate force tensor, and isotropic hardening/softening conjugate relation, respectively. It is noted that c_1^d and c_2^d can be determined using experimental in-plane shear strength-strain data explained in (Barbero 2001). Using these equations, damage potential and damage evolution laws can be defined which are presented in the following sections.

1.4 Damage conditions

Associative damage can be used here to derive the evolution equations for the constitutive model such that the damage potential, G, is equal to the damage criterion, g. Analogous to plasticity, it is postulated that damaging behavior can be distinguished from non-damaging behavior on a local basis by a damage surface of the form of (Barbero 2001)

$$G = g(\mathbf{Y}, \kappa) = \sqrt{\mathbf{Y}.\mathbf{J}.\mathbf{Y}} - (K(\kappa) - K_0) \tag{12}$$

where $K(\kappa)$ is defied previously in Eq. (11), the $\mathbf{J}$ tensor is determined by available data on a single composite lamina, and K_0 is the initial damage threshold at which damage begins to occur (Barbero 2001). Also in Eq. (12), the Y_i are eigenvalues of damage conjugate force tensor defied in Eq. (10). $g(\mathbf{Y}, \kappa) < 0$ indicates a non-damaging state, $g(\mathbf{Y}, \kappa) = 0$ indicates a damage inducing state, and $g(\mathbf{Y}, \kappa) > 0$ is understood to be inadmissible.

1.5 Damage evolution equations

Damage evolution equations can be obtained from dissipation potential function. If the potential function is chosen to define convex surface containing the origin of the forces space, then the satisfaction of the second law of thermodynamics, Clausius-Duhem's inequalities, is be assured in the local form. The energy dissipation due to damage are found by substituting the thermodynamic state laws into the Clausius-Duhem inequality and are thus given as the product of the thermodynamic conjugate forces with the respective flux variables as follows

$$\Pi = \boldsymbol{\sigma}:\dot{\boldsymbol{\varepsilon}}^{id} - \mathbf{Y}:\dot{\boldsymbol{\varphi}} - \rho K.\dot{\kappa} - \mathbf{q}.\frac{\nabla T}{T} \geq 0 \tag{13}$$

ρ is the mass density, $\mathbf{q}$ is the heat flux vector, ∇T is the temperature gradient, and dot over the parameters is the time derivative of parameters. Also, $\boldsymbol{\varepsilon}^{id}$ is inelastic-damage part of the strain tensor. Using the theory of functions of several variables, damage Lagrange multiplier $\dot{\lambda}^{d}$ is utilized to construct the objective function Ω in the following form

$$\Omega = \Pi - G\dot{\lambda}^{d} \tag{14}$$

where G is the damage potential. In order to obtain the damage tensor rate, and deriving evolution equations for the hardening state variables, the following conditions are used to extremize the objective function

$$\frac{\partial \Omega}{\partial \boldsymbol{\sigma}} = 0; \quad \frac{\partial \Omega}{\partial \mathbf{Y}} = 0; \quad \frac{\partial \Omega}{\partial K} = 0 \tag{15}$$

when $G \geq 0$, the corresponding evolution equations for the damage tensor, and the corresponding hardening state variables, are given as follows

$$\dot{\boldsymbol{\varepsilon}}^{id} = +\frac{\partial G}{\partial \boldsymbol{\sigma}}\dot{\lambda}^{d}; \quad \dot{\boldsymbol{\varphi}} = -\frac{\partial G}{\partial \mathbf{Y}}\dot{\lambda}^{d}; \quad \dot{\kappa} = -\frac{\partial G}{\partial K}\dot{\lambda}^{d} \tag{16}$$

The following loading-unloading conditions known as the Kuhn-Tucker optimality conditions must also be enforced (Voyiadjis 2000 and 2007).

$$\dot{\lambda}^{d} \geq 0; \quad G \leq 0; \quad \dot{\lambda}^{d} G = 0 \tag{17}$$

1.6 Stress Integration algorithm

In the solution procedure, a linearized form of the governing equation is solved within an incremental iterative Newton-Raphson solution procedure for the increment of strain over the time increment Δt_j such that (Voyiadjis 2007)

$$\boldsymbol{\varepsilon}_j = \boldsymbol{\varepsilon}_o + \Delta t_j d\boldsymbol{\varepsilon} = \boldsymbol{\varepsilon}_o + \Delta \boldsymbol{\varepsilon}_j \tag{18}$$

where the subscripted j and 0 indicate that the variable is computed at iteration j and at the previously converged state, respectively; and the symbol Δ denotes a total increment from the previously converged state to the iteration, j. The increments of the damage multiplier, $\Delta\lambda_j^{d}$, must be computed, and then the state variables are updated using Eq. (16)

$$\boldsymbol{\varepsilon}_j^{id} = \boldsymbol{\varepsilon}_o^{id} + \Delta\boldsymbol{\varepsilon}_j^{id}; \quad \boldsymbol{\varphi}_j = \boldsymbol{\varphi}_o + \Delta\boldsymbol{\varphi}_j; \quad \kappa_j = \kappa_o + \Delta\kappa_j \tag{19}$$

The $\boldsymbol{\sigma}$ and $\mathbf{Y}$ for this integration scheme are defined at jth iteration as follows

$$\boldsymbol{\sigma}_j = \mathbf{C}^{e}:(\boldsymbol{\varepsilon}_j - \boldsymbol{\varepsilon}_j^{id}) = \boldsymbol{\sigma}_o + \mathbf{C}_j^{e}:(\Delta\boldsymbol{\varepsilon}_j - \Delta\boldsymbol{\varepsilon}_j^{id}) + \mathbf{C}_j^{e}:\left(\mathbf{C}^{-e}:\frac{\partial \mathbf{C}^{e}}{\partial \boldsymbol{\varphi}}:(\boldsymbol{\varepsilon} - \boldsymbol{\varepsilon}^{id})\right)_j:\Delta\boldsymbol{\varphi}_j \tag{20}$$

$$\mathbf{Y}_j = \boldsymbol{\sigma}_j^{T}:\left(\frac{\partial \mathbf{C}^{-e}}{\partial \boldsymbol{\varphi}}\right)_j:\boldsymbol{\sigma}_j \tag{21}$$

The integration scheme used here enforces that $g_j = 0$ at the end of the time step

$$g_j = g(\mathbf{Y}_j, \kappa_j) = \sqrt{\mathbf{Y}_j.\mathbf{J}.\mathbf{Y}_j} - (K(\kappa_j) - K_0) = 0 \tag{22}$$

In order to address this type of problem, a return-mapping algorithm is used. This algorithm has an initial elastic-predictor step, followed by a damage-corrector step. In the elastic-predictor step, the incremental strains are assumed to be elastic with no damage increment such that an initial trial stress and an initial trial damage conjugate force can be computed as

$$\boldsymbol{\sigma}_j^{trial} = \boldsymbol{\sigma}_o + \mathbf{C}_o^e:\Delta\boldsymbol{\varepsilon}_j \tag{23}$$

$$\mathbf{Y}_j^{trial} = \boldsymbol{\sigma}_j^{trial}:\left(\frac{\partial \mathbf{C}^{-e}}{\partial \boldsymbol{\varphi}}\right)_j:\boldsymbol{\sigma}_j^{trial} \tag{24}$$

The trial state $(\boldsymbol{\sigma}_j^{trial}, \mathbf{Y}_j^{trial}, \boldsymbol{\varepsilon}_o^{id}, \boldsymbol{\varphi}_o, \kappa_o)$ is then used in a trial damage criterion to decide whether an elastic point enters the damage regimes or whether a damage point elastically unloads. For the case when $g^{trial} < 0$, the integration point is assumed to be elastic with no additional damage and the current state of $(\boldsymbol{\sigma}_j, \mathbf{Y}_j, \boldsymbol{\varepsilon}_o^{id}, \boldsymbol{\varphi}_o, \kappa_o)$ is equal to the trial state of $(\boldsymbol{\sigma}_j^{trial}, \mathbf{Y}_j^{trial}, \boldsymbol{\varepsilon}_o^{id}, \boldsymbol{\varphi}_o, \kappa_o)$. When $g^{trial} > 0$, the current state resulting from this trial state lies outside of the damage surface. Damage has occurred and the state has to be returned to the damage surface.

1.7 Layer-wise finite element formulation in conjunction with CDM

Considering a laminated plate composed of N orthotropic lamina, each being arbitrarily oriented with respect to the laminate (x, y) coordinates. The coordinate center is taken to be in the mid-plane of the laminate, z is through the thickness and (x, y) are in-plane coordinates. The displacements (u_1, u_2, u_3) correspond to the (x, y, z) directions at each point in the laminate are assumed to be in the form of (Barbero 1990)

$$\begin{aligned} u_1(x,y,z) &= u(x,y) + U(x,y,z) \\ u_2(x,y,z) &= v(x,y) + V(x,y,z) \\ u_3(x,y,z) &= w(x,y) \end{aligned} \tag{25}$$

where (u, v, w) are the displacement components of a point $(x, y, 0)$ on the reference plane of the laminate, and U and V are functions which vanish on the reference plane as $U(x,y,0) = V(x,y,0) = 0$. Also U and V can be approximated as

$$\begin{aligned} U(x,y,z) &= \sum_{m=1}^{n} U^m(x,y)\phi^m(z) \\ V(x,y,0) &= \sum_{m=1}^{n} V^m(x,y)\phi^m(z) \end{aligned} \tag{26}$$

where U^m, and V^m are undetermined coefficients, and ϕ^m are any continuous functions that satisfy the condition $\phi^m(0) = 0$ for all $m = 1, 2, \ldots, n$. For example, a finite element approximation based on the Lagrangian interpolation through the thickness can be obtained from Eq. (26) considering the $n = pN + 1$, where N is the number of layers through the thickness, p is the degree of the interpolation polynomials of $\phi^m(z)$. The approximation in Eq. (25) can also be viewed as the global semi-discrete finite element approximations of U and V through the thickness. In that case ϕ^m

denote the through thickness interpolation functions, and U^m, and V^m, are the global nodal values of U and V at the nodes through the thickness of the laminate. Note that the transverse deflection here is assumed to be independent of the thickness coordinate, which leads to neglect the transverse normal stress.

In order to understand the relation between the nodal resultant forces of laminate and displacements in layer-wise plate theory, the first variation of potential energy, equilibrium condition, is expanded as follows

$$\delta\Pi = \frac{1}{2}\int_A \left\{ N_x\left(\frac{\partial \delta u}{\partial x}\right) + N_y\left(\frac{\partial \delta v}{\partial v}\right) + N_{xy}\left(\frac{\partial \delta u}{\partial y} + \frac{\partial \delta v}{\partial x}\right) + Q_x\frac{\partial \delta w}{\partial x} + Q_y\frac{\partial \delta w}{\partial y} \right.$$
$$\left. + \sum_{m=1}^{N}\left[N_x^m\left(\frac{\partial \delta U^m}{\partial x}\right) + N_y^m\left(\frac{\partial \delta V^m}{\partial y}\right) + N_{xy}^m\left(\frac{\partial \delta U^m}{\partial y} + \frac{\partial \delta V^m}{\partial x}\right) + Q_x^m \delta U^m + Q_y^m \delta V^m \right] \right\} dA = 0 \tag{27}$$

where the resultant forces of the laminate are

$$\begin{aligned} N_x, N_y, N_{xy} &= \int_{-h/2}^{h/2} (\sigma_x, \sigma_y, \sigma_{xy}) dz \\ Q_x, Q_y &= \int_{-h/2}^{h/2} (\sigma_{xz}, \sigma_{yz}) dz \\ N_x^m, N_y^m, N_{xy}^m &= \int_{-h/2}^{h/2} (\sigma_x, \sigma_y, \sigma_{xy}) \phi^m(z) dz \\ Q_x^m, Q_y^m &= \int_{-h/2}^{h/2} (\sigma_{xz}, \sigma_{yz}) \frac{d\phi^m(z)}{dz} dz \end{aligned} \tag{28}$$

σ_x, σ_y, σ_{xy}, σ_{xz}, and σ_{yz} are the stress components. The constitutive equations of the laminate in damage state are given by

$$\begin{aligned} \{\mathbf{N}\} &= [\mathbf{A}]^{(a\lg)}\{\mathbf{e}\} + \sum_{k=1}^{N}[\mathbf{B}^m]^{(a\lg)}\{\mathbf{e}^m\} \\ \{\mathbf{N}^m\} &= [\mathbf{B}^m]^{(a\lg)}\{\mathbf{e}\} + \sum_{k=1}^{N}[\mathbf{D}^{mr}]^{(a\lg)}\{\mathbf{e}^m\} \end{aligned} \tag{29}$$

where $\{e\}$ and $\{e^m\}$ are the in-plane and layers interfaces strain vectors respectively, and $[A]^{(a\lg)}$, $[D^{mr}]^{(a\lg)}$, and $[B^m]^{(a\lg)}$ are extensional, bending stiffness, and bending-extensional coupling stiffness matrices respectively, defined as follows

$$\begin{aligned} &\text{if} \quad (p,q = 1,2,6) && ; \quad \text{if} \quad (p,q = 4,5) \\ &A_{pq}^{(a\lg)} = \sum_{k=1}^{N}\int_{z_k}^{z_{k+1}} C_{pq}^{(a\lg)^k} dz && ; \quad A_{pq}^{(a\lg)} = \sum_{k=1}^{N}\int_{z_k}^{z_{k+1}} C_{pq}^{(a\lg)^k} dz \\ &B_{pq}^{(a\lg)^m} = \sum_{k=1}^{N}\int_{z_k}^{z_{k+1}} C_{pq}^{(a\lg)^k} \phi^m dz && ; \quad B_{pq}^{(a\lg)^m} = \sum_{k=1}^{N}\int_{z_k}^{z_{k+1}} C_{pq}^{(a\lg)^k} \frac{d\phi^m}{dz} dz \\ &D_{pq}^{(a\lg)^{mr}} = \sum_{k=1}^{N}\int_{z_k}^{z_{k+1}} C_{pq}^{(a\lg)^k} \phi^m \phi^r dz && ; \quad D_{pq}^{(a\lg)^{mr}} = \sum_{k=1}^{N}\int_{z_k}^{z_{k+1}} C_{pq}^{(a\lg)^k} \frac{d\phi^m}{dz}\frac{d\phi^r}{dz} dz \end{aligned} \tag{30}$$

where $C_{pq}^{(a\lg)}$ is elastic-damage reduced stiffness matrix. In the case of pure elastic behavior, $C_{pq}^{(a\lg)}$ should be replaced by the elastic stiffness tensor, and Q_{pq} defined in mechanics of composite materials. The local stresses in each constituent can be obtained from the applied loading increment by using the assumption of the lamination theory.

Integration in the thickness direction is performed using linear variation; two points at the top and bottom of each numerical layer are considered for calculation of stiffness properties through the thickness. If the piecewise linear functions through the thickness of the laminate are considered for damage effects, the following explicit relations can be obtained for the coefficients of the laminate stiffness matrices.

$$
\begin{aligned}
&A^{(a\lg)}{}_{pq} = \sum_{k=1}^{N} \frac{1}{2}\left({}^{T}C^{(a\lg)k}{}_{pq} + {}^{B}C^{(a\lg)k}{}_{pq}\right) t_k && p,q = 1,2,4,5,6 \\
&B^{(a\lg)m}{}_{pq} = \left(\frac{{}^{T}C^{(a\lg)m-1}{}_{pq}}{3} + \frac{{}^{B}C^{(a\lg)m-1}{}_{pq}}{6}\right) t^{m-1} + \left(\frac{{}^{T}C^{(a\lg)m}{}_{pq}}{6} + \frac{{}^{B}C^{(a\lg)m}{}_{pq}}{3}\right) t^{m} && p,q = 1,2,6 \\
&B^{(a\lg)m}{}_{pq} = \frac{1}{2}\left({}^{T}C^{(a\lg)m-1}{}_{pq} + {}^{B}C^{(a\lg)m-1}{}_{pq}\right) - \frac{1}{2}\left({}^{T}C^{(a\lg)m}{}_{pq} + {}^{B}C^{(a\lg)m}{}_{pq}\right) && p,q = 4,5 \\
&D^{(a\lg)mm}{}_{pq} = \left(\frac{{}^{T}C^{(a\lg)m-1}{}_{pq}}{4} + \frac{{}^{B}C^{(a\lg)m-1}{}_{pq}}{12}\right) t^{m-1} + \left(\frac{{}^{T}C^{(a\lg)m}{}_{pq}}{12} + \frac{{}^{B}C^{(a\lg)m}{}_{pq}}{4}\right) t^{m} && p,q = 1,2,6 \\
&D^{(a\lg)mm}{}_{pq} = \left(\frac{{}^{T}C^{(a\lg)m-1}{}_{pq} + {}^{B}C^{(a\lg)m-1}{}_{pq}}{2t^{m-1}}\right) + \left(\frac{{}^{T}C^{(a\lg)m}{}_{pq} + {}^{B}C^{(a\lg)m}{}_{pq}}{2t^{m}}\right) && p,q = 4,5 \\
&D^{(a\lg)mr}{}_{pq} = D^{(a\lg)rm}{}_{pq} = \left({}^{T}C^{(a\lg)m}{}_{pq} + {}^{B}C^{(a\lg)m}{}_{pq}\right)\frac{t^{m}}{12} && p,q = 1,2,6 \\
&D^{(a\lg)mr}{}_{pq} = D^{(a\lg)rm}{}_{pq} = -\left(\frac{{}^{T}C^{(a\lg)m}{}_{pq} + {}^{B}C^{(a\lg)m}{}_{pq}}{t^{m}}\right) && p,q = 4,5
\end{aligned}
\tag{31}
$$

where the coefficients are computed in terms of the damage values of the reduced stiffness coefficients in global coordinates and superscripts T and B refer to top and bottom of each layer, respectively.

In the incremental form, the weak form of the equilibrium equation with the elastic-damaged material stiffness matrix at j[th] time step is as follows

$$\int_{v} \delta\boldsymbol{\varepsilon}:\mathbf{C}_j^{ed}:d\boldsymbol{\varepsilon}_j dV = -\int_{v} \delta\mathbf{u}:\mathbf{b}_j dV - \int_{\Gamma_t} \delta\mathbf{u}:\hat{\mathbf{t}}_j d\Gamma - \int_{V} \delta\boldsymbol{\varepsilon}:\boldsymbol{\sigma}_j dV \tag{32}$$

where $\boldsymbol{\varepsilon}$, $\mathbf{C}^{ed}$, $\boldsymbol{\sigma}$, $\mathbf{u}$, $\mathbf{b}$, $\hat{\mathbf{t}}$, and V are strain vector, material stiffness matrix, stress vector, displacement vector, body inertia force vector, traction external force vector, and total volume of body respectively. Note that this equation is enforced over the entire body, including both the damage and elastic domains. In the right hand side of the governing equations, the stress at j[th] iteration must be known. It was explained in the integration scheme, that for each integration point in an inelastic state, the implicit backward Euler elastic predictor-inelastic corrector algorithm is used to compute the stress. The governing equation can be linearized consistently and solved within an incremental iterative Newton-Raphson solution procedure.

The displacement filed, u_j, is discretized using layer-wise plate theory. The interpolating relation is defined as follows

$$u_j = [\psi]\begin{Bmatrix}\Delta \\ \Delta^m\end{Bmatrix}_j, \quad \{\Delta\} = \begin{Bmatrix}u \\ v \\ w\end{Bmatrix}, \quad \{\Delta^m\} = \begin{Bmatrix}U^m \\ V^m\end{Bmatrix}, \quad [\psi] = \begin{bmatrix}[N] & 0 \\ 0 & [\phi^m]\end{bmatrix} \tag{33}$$

where $[N]$ and $[\phi^m]$ contains the in-plane and through the thickness set of nodal elements of the well-known finite element shape functions, respectively. Also (u, v, w) and (U^m, V^m) are mid-plane and numerical layers nodal displacements, respectively. By taking the required derivatives, the strains are obtained using the following strain-displacement relation

$$\boldsymbol{\varepsilon}_j = [\mathbf{B}]\{\mathbf{u}\}_j; \; \boldsymbol{\varepsilon}_j = \begin{Bmatrix}\mathbf{e}_j \\ \mathbf{e}_j^m\end{Bmatrix}; \quad \mathbf{e}_j = [\mathbf{B}_L][\Delta]; \; \mathbf{e}_j^m = [\overline{\mathbf{B}}_L][\Delta^m] \tag{34}$$

$$[\mathbf{B}] = \begin{bmatrix}[\mathbf{B}_L] & 0 \\ 0 & [\overline{\mathbf{B}}_L]\end{bmatrix} \tag{35}$$

where $[\mathbf{B}_L]$ and $[\overline{\mathbf{B}}_L]$ are matrices of shape function derivatives of mid-plane and numerical layers degree of freedom respectively. Using this discretization, the weak form of the equilibrium equation becomes

$$\begin{aligned}&\{\delta\mathbf{u}\}_j^T \int_{\Gamma_t} [\mathbf{B}]^T [\mathbf{E}^{ed}]_j^{a\lg} [\mathbf{B}]\{d\mathbf{u}\} d\Gamma \\ &= \{\delta\mathbf{u}\}_j^T \Big(\int_V [\psi]^T \{\mathbf{b}\}_j dV + \int_{\Gamma_t} [\psi]^T \{\hat{\mathbf{t}}\}_j d\Gamma - \int_V [\mathbf{B}]^T \{\boldsymbol{\sigma}\}_j dV \Big)\end{aligned} \tag{36}$$

where $[\mathbf{E}^{ed}]_j^{a\lg}$ is

$$[\mathbf{E}^{ed}]_j^{a\lg} = \begin{bmatrix}[\mathbf{A}]_j^{(a\lg)} & [\mathbf{B}^m]_j^{(a\lg)} \\ [\mathbf{B}^m]_j^{(a\lg)} & [\mathbf{D}^{mr}]_j^{(a\lg)}\end{bmatrix} \tag{37}$$

It is noted that transpose of matrix $[\mathbf{B}]^T$ is specially defined as follows

$$[\mathbf{B}]^T = \begin{bmatrix}[\mathbf{B}_L]^T & 0 \\ 0 & [\overline{\mathbf{B}}_L]^T\end{bmatrix} \tag{38}$$

This governing equation must be admissible for any displacement variation, which can be written as a set of algebraic equations

$$[K]^{ed}\{du\}_j = \{f^{\text{ext}}\} + \{f^{\text{int}}\} + \{f^b\} \tag{39}$$

where the sub-matrices are defined as follows

$$\text{Stiffness matrix:} \qquad [K]^{ed} = \int_{\Gamma_t} [B]^T [E^{ed}]_j^{a\lg} [B] d\Gamma \tag{40}$$

External forces vector: $$\{f^{\text{ext}}\} = \int_{\Gamma_t}[\psi]^T\{\hat{\mathbf{t}}\}_j d\Gamma \tag{41}$$

Body forces vector : $$\{f^b\} = \int_V[\psi]^T\{b\}_j dV \tag{42}$$

Internal forces vector: $$\{f^{\text{int}}\} = -\int_V[B]^T\{\sigma\}_j dV \tag{43}$$

Using layer-wise lamination theory and finite element procedure, the stiffness matrix and its sub-matrices are obtained

$$[K]^{ed} = \begin{bmatrix} [k^{11}] & [k_1^{12}] & \dots & [k_N^{12}] \\ [k_1^{11}] & [k_{11}^{12}] & \dots & [k_{1N}^{22}] \\ . & . & \dots & . \\ [k_N^{21}] & [k_{N1}^{22}] & \dots & [k_{NN}^{22}] \end{bmatrix} \tag{44}$$

where the sub-matrices $[k^{11}], [k_m^{12}], [k_m^{21}]$, and $[k_{mr}^{22}]$ are as follows

$$\begin{aligned}
[K^{11}] &= \Sigma_e \int_{\Gamma e}([B_L]^T[A]^{(a\lg)}[B_L])d\Gamma_e \\
[K_m^{12}] &= \Sigma_e \int_{\Gamma e}([B_L]^T[B^m]^{(a\lg)}[\overline{B}_L])d\Gamma_e \qquad m = 1,2,3,\dots,N \\
[K_m^{21}] &= \Sigma_e \int_{\Gamma e}([\overline{B}_L]^T[B^m]^{(a\lg)}[B_L])d\Gamma_e \qquad m = 1,2,3,\dots,N \\
[K_{mr}^{22}] &= \Sigma_e \int_{\Gamma e}([\overline{B}_L]^T[D^{mr}]^{(a\lg)}[\overline{B}_L])d\Gamma_e \qquad m,r = 1,2,3,\dots,N
\end{aligned} \tag{45}$$

These matrices and vectors can be computed for the elements and then implemented into the global matrices and vectors for the entire body. A finite element procedure is then followed to solve the equations. The problem defined by these equations is nonlinear as the stiffness and the residual loads depend on the deformations. An iterative procedure is required to solve the problem. The nodal forces are produced by the stress field that satisfies the elasto-damage conditions. The difference between these forces and the applied ones gives the residual forces. During a load increment, an element or part of that may prone to damage. All stresses and strains quantities are calculated and monitored at each Gaussian integration point and therefore the damage occurrence can be determined at such points. Consequently, an element may have partially elastic and partially damage behavior. For any load increment, it is necessary to determine which portion of that is in elastic condition and which part is in damage condition. Then the stress and strain terms are adjusted until satisfaction of the damage criterion. It is noted that the layer-wise element uses a reduced constitutive matrix that is stored as a full 6×6 matrix where its transverse normal components are set to zero; therefore, the layer-wise element can directly utilize the full 3-D damage mechanics equations in the original form.

For more understanding of the solution procedure, the main steps of the developed computer program to analyze the elastic-damage behavior of the laminates are explained as follows:

1- Defining the problem parameters such as geometry, boundary conditions, loading conditions, load increments functions, material stiffness and strength properties, mesh parameters, and etc.
2- Imposing the j^th load increment.
3- Setting the $\Delta\lambda_j^{d(0)} = 0$; $\varepsilon_j^{id(0)} = \varepsilon_{j-1}^{id}$; $\varphi_j^{(0)} = \varphi_{j-1}$; $\kappa_j^{(0)} = \kappa_{j-1}$
4- Compute the algorithmic consistent tangent stiffness matrix of each gauss points using.
5- Compute the element stiffness matrix of each element by considering the step (4) and constructing sparse global stiffness matrix.
6- Solving the linearized Eq. (39) and obtaining the displacement field increment.
7- Computing the strains and stresses according to the current load increment at each gauss points in local material coordinate system in each numerical layer, and accumulating with the previous converged strain-stress fields.
8- Checking the damage condition. If damage occurs then perform the damage corrector using the fully implicit backward Euler return-mapping algorithm.
9- Updating the state variables such as $\Delta\lambda_j^d$, σ_j, ε_j^{id}, φ_j, κ_j
10- Computing the nodal internal forces of each element using the last updated stress and calculating residual forces at each gauss point.
11- Checking the force and displacement convergence criteria of the overall problem. If they are satisfied then go to the next loading increment; otherwise replace the residual forces in initial incremental load of this step and go to the next iteration in Step (4).
12- Repeating the step (2) to step (11) until the total load is applied and all state variables return to the damage surface.

2. Numerical examples

In this section a set of numerical examples are performed to discuss about the results obtained from the developed program and procedure. The example involve angle-ply laminate tensile test specimens that exhibit damage localization due to the free edge effect without considerable normal stress (in the thickness direction) caused by free edges.

For this example, the fiber-reinforced composite material used for each of the four plies are described by the following set of homogenized material coefficients. Elastic constants for the un-damaged composite material are $E_{11} = 167$ GPa; $E_{22} = E_{33} = 8.13$ GPa; $\nu_{12} = \nu_{13} = \nu_{23} = 0.27$; $G_{12} = G_{13} = G_{23} = 8.8252$ GPa. Damage surface and hardening constants using Barbero *et al.* (2001) approach are $J_{11} = 0.9524\text{e-}15$; $J_{22} = J_{33} = 0.4381\text{e-}12$. ; $c_1^d = 7.595\text{e-}7$, and $\gamma(0) \cong 0.0$.

A symmetric angle-ply laminate tensile test specimen is chosen as a representative of problems that exhibit localized stress concentration and damage evolution. The presence of free edges in laminated composites introduces an additional level of complexity. The state of stress in the vicinity of the free edges is three-dimensional, with nonzero through-thickness stresses. The through-thickness stresses include the interlaminar normal stress, σ_z, and two interlaminar shear stresses.

Insight into the influence of fiber orientation and stacking sequence on interlaminar stresses can be obtained through a study of through-thickness distribution of the interlaminar shear forces and moment. Distributions of interlaminar forces and moment for the adjacent layers of angle-ply laminates are shown that the only nonzero force and moment is the interlaminar force in the *x-z* plane. Herakovick (1998) showed that, it varies linearly through each layer and exhibits identical maximum magnitudes at each $+\theta/-\theta$ interface. In the real material that exhibit inelastic response associated with matrix plasticity and damage as contrasted with the idealized linear elastic material under consideration, the interlaminar stresses are not singular, but they do exhibit very large gradients near the free edges.

Fig. 2(a) shows the geometry and boundary conditions for a symmetric angle-ply laminate tensile test specimen with the lay-up configurations of $[+\theta/-\theta]_s$. Three different lay-ups of $[+15/-15]_s$, $[+30/-30]_s$, and $[+45/-45]_s$ are considered. The specimens are loaded by imposing a uniform axial displacement at the end $x = L$, while the axial displacement is constrained at $x = -L$. The imposed axial displacement is increased in a series of non-uniformly load steps until one of the damage eigenvalues achieving a value of unity indicating a local material failure Fig. 2(b) shows the 2-D mesh of 8-node quadratic elements used to model the specimen. The mesh consists of uniform distribution of 6 elements along the length of the specimen; however, the refinement level is purposely varied across the width of the specimen. The size of the elements are varied across the width of the specimen from $y = -W$ to $y = W$. The element widths are $t_L/16$, $t_L/16$, $t_L/8$, $t_L/4$, $t_L/2$, t_L, t_L, $2t_L$, $3t_L$, $3t_L$, $2t_L$, t_L, t_L, $t_L/2$, $t_L/4$, $t_L/8$, $t_L/16$, and $t_L/16$ that t_L is the thickness of a single material layer of the laminate. This non-uniform mesh is chosen to permit the free edge interlaminar stresses to be resolved along the lateral edge at $y = W$ and $y = -W$. The 2-D mesh shown in Fig. 2(b) is used in conjunction with three different discretizations of 2, 4 and 6 per material layer through the thickness of laminate in order to illustrate the effect of discretizations on the progressive damage response. All models are capable of resolving the free edge stress concentrations; however, the accuracy that they can meet depends on the level of the employed transverse discretizations. Considering the laminates with four layers and using six discretizations at each material layer leads to the FEM modeling with 24 elements through the thickness. Then using the number of 108 elements for in-plane mesh, the total number of 2592 elements was used for each model, which

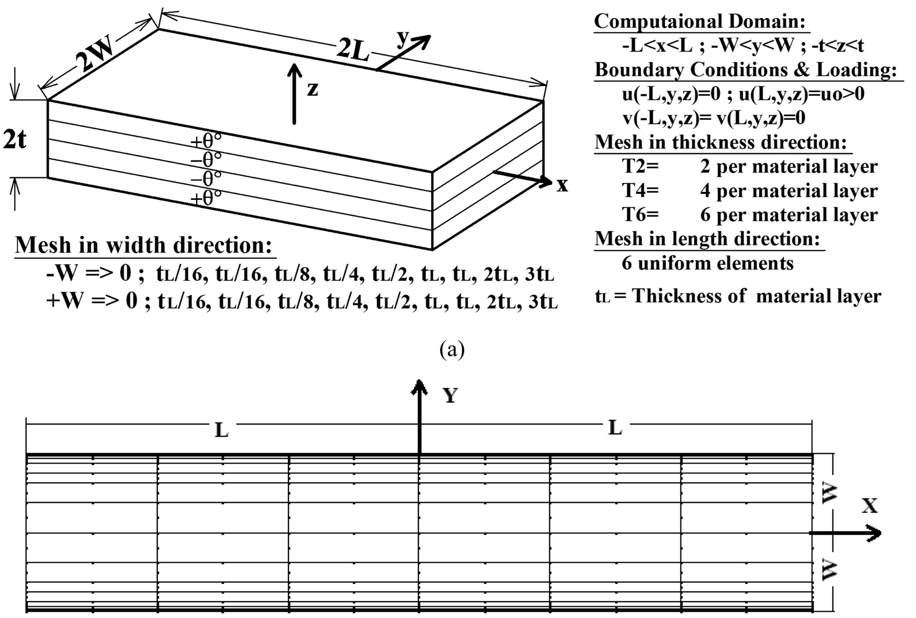

(a)

(b)

Fig. 2 Geometry, loading, boundary conditions and FEM mesh of a typical laminate make the nonlinear analyses quite time consuming.

Fig. 3 shows the distribution of damage eigenvalues through the thickness of a laminate with the lay-up of $[+45/-45]_s$ for various number of discritizations at each material layer. These results are obtained for free edges at the point of $x = L/3$ and $y = W$. This figure shows that the maximum values of both damage parameters occur at the interface of +45/-45 layers. It also shows that with increasing the number of discritizations, the maximum damage eigenvalues are increased which indicating that by refining the discritization, the obtained damage values at +45/-45 interfaces approach to unity and may cause debounding between the layers. In the present study, the maximum of six discritizations through the each material layer were used due to the CPU time limitation. It is noted that when $\varphi_2 = 1.0$ the shearing delamination modes can be activated, however, by $\varphi_3 = 1.0$ the normal or opening delamination mode can be occurred. When the refined discritizations are applied, the values of φ_3 through the thickness of the laminate tend to zero value except at the interfaces of +45/-45 layers which are rapidly increased as shown in Fig. 3(b). The sudden increase of the damage parameter at the interfaces of +45/-45 layers is also observed for φ_2 in Fig. 3(a). This behavior is due to the almost singular nature of the stresses at the free edges of these interfaces.

Variation of maximum damage eigenvalues versus the average applied strain for various symmetric angle ply laminates at free edges are depicted in Fig. 4. Fig. 4(a) indicates that the maximum values of φ_2 obtained for the lay-up of [+30/-30] are very close to those obtained for [+15/-15]. The obtained damage eigenvalues of φ_3 are smaller than those obtained for φ_2 for the lay-up of [+45/-45]. The increasing rate of φ_3 damage values obtained for [+15/-15] lay-up is significantly larger than the rate of φ_2 and φ_3 of the other lay-ups.

Fig. 5 shows the distribution of damage eigenvalues through the width of the laminates with various lay-ups of [+15/-15]s, [+30/-30]s and [+45/-45]s at the $\theta/-\theta$ layers interfaces. Fig. 5(a) shows that the obtained values of φ_2 for the lay-ups of [+30/-30]s and [+45/-45]s are larger than those obtained for [+15/-15]s. This phenomenon leads to the higher spreading of matrix cracks in the lay-ups of [+30/-30]s and [+45/-45]s. This figure also shows that in the area of about 0.15W in the vicinity of the free edge boundaries, the in-plane transverse eigenvalues are rapidly increased for the lay-ups of [+30/-30]s and [+45/-45]s indicating the free edge effects on φ_2. These free edge effects are not significant for the lay-up of [+15/-15]s.

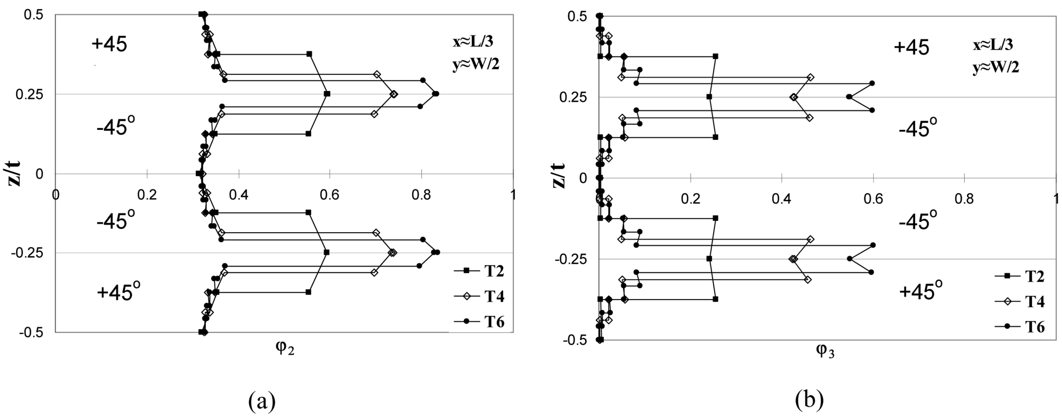

Fig. 3 Distribution of damage eigenvalues through the thickness of laminate with lay-up of [+45/-45]s with various number of discritization for each material layer; (a) φ_2, (b) φ_3

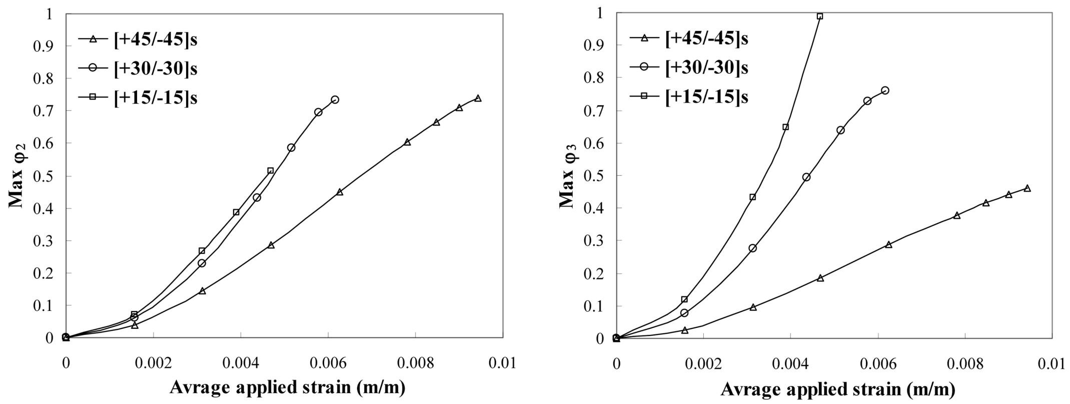

(a) (b)

Fig. 4 Variation of maximum damage eigenvalues versus the average applied strain for various symmetric angle ply laminates at free edges; (a) φ_2, (b) φ_3

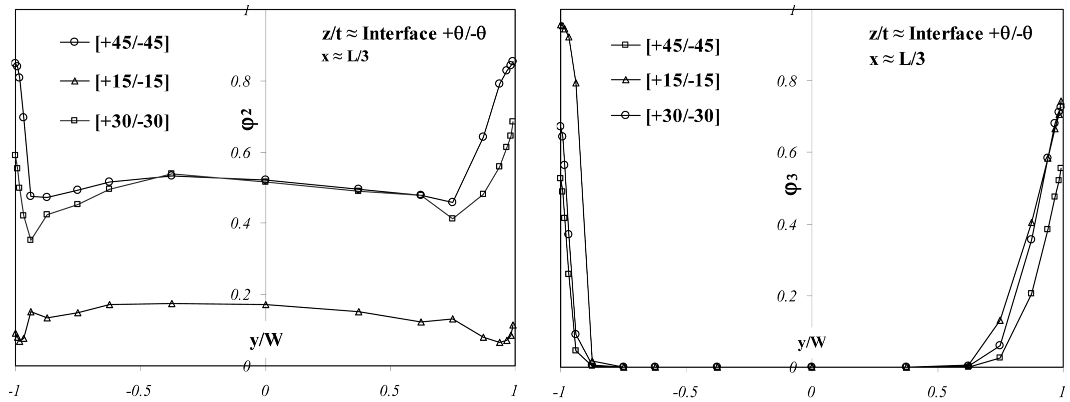

(a) (b)

Fig. 5 Distribution of damage eigenvalues through the width of laminates with various lay-ups between the θ/-θ layers interfaces; (a) φ_2, (b) φ_3

Fig. 5(b) shows that the values of φ_3 are almost zero through the width of the laminates except for the free edge effect zone which they are suddenly increased. The values of φ_3 for the lay-up of [+15/-15]s in the vicinity of the free edges are larger than those obtained for [+30/-30]s and [+45/-45]s. In this way, all of the angle ply laminates, specially [+15/-15]s tend to delaminate between +θ/-θ layers at the free edges.

Considering the distribution and values of the damage eigenvalues, it can be concluded that the dominant damage mechanism in the lay-ups of [+30/-30]s and [+45/-45]s is matrix cracking. However, the lay-up of [+15/-15] may be delaminated in the vicinity of the edges and at +θ/-θ layers interfaces.

Fig. 6(a) shows the convergence of the average stress-strain behaviour for [+45/-45]s laminate with various number of divisions through the thickness of each material layer. It shows that the obtained results using 4 and 6 number of discretizations for each material layer are very close to

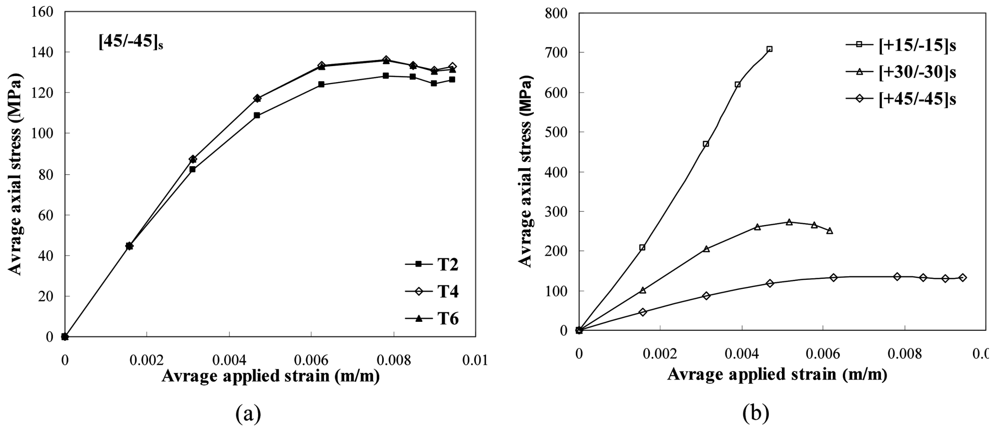

Fig. 6 Average axial stress versus the applied strain; (a) effects of through the thickness discretization (b) various symmetric angle ply laminates

each other. However, using the 2 number of discretizations leads to under estimate the results. It may be concluded that using 4 numerical layers through the thickness of each material layer, is enough to produce the acceptable results.

Variations of the average stress versus the average applied strain for different symmetric angle ply laminates are shown in Fig. 6(b). It shows that the axial stiffness and failure stress obtained for the lay-up of [+15/-15]s are larger than those obtained for the other two lay-ups. In this lay-up, by increasing the applied axial strain, the resultant axial stress is increased without significant stiffness reduction up to the final failure of the laminate. In contrast, for the lay-ups of [+30/-30]s and [+45/-45]s, the stiffness reduction plays an important role in stress-strain behavior. These facts can be explained considering Fig. 5. The presented results in this figure showed that the matrix cracks are widely developed for the lay-ups of [+30/-30]s and [+45/-45]s, and therefore caused the overall stiffness reduction. But, for the lay-up of [+15/-15]s, the dominant damage mode is φ_3 which cause delamination between +15/-15 layers interface and may yield an unstable delamination propagation near the final failure load. It is known that the delamination has not considerable effect on the axial stiffness reduction as was explained for [+15/-15]s lay-up stress-strain behavior in Fig. 6(b).

3. Conclusions

A 3-D continuum damage mechanics formulation for composite laminates and its implementation into a finite element model that is based on the layer-wise laminate plate theory was described. Details of the numerical implementation of the 3-D CDM model into the layer-wise finite element model were also performed. The progressive damage of different angle ply composite laminates under quasi-static loading that exhibit the free edge effects were investigated. It was shown that in the area of about 0.2W in the vicinity of the free edge boundaries, the in-plane transverse eigenvalues are rapidly increased for the lay-ups of [+30/-30]s and [+45/-45]s indicating the free edge effects. These free edge effects are not significant for the lay-up of [+15/-15]s. The obtained through the thickness damage eigenvalues were smaller than those obtained for transverse eigenvalues for the lay-up of [+45/-45]. The increasing rate of through the thickness damage values obtained for [+15/-15] lay-up were rapidly tend to unity. Considering the distribution and values of the damage eigenvalues, it was concluded that the dominant damage mechanism in the lay-ups of [+30/-30]s and [+45/-45]s is matrix cracking. However, the lay-up of [+15/-15] may be delaminated in the vicinity of the edges and at $+\theta/-\theta$ layers interfaces.

References

Allix, O. and Ladeveze, P. (1989), "A damage prediction method for composite structures", *Int. J. Numer. Meth. Eng.,* **27**, 271-283.

Allix, O. and Ladeveze, P. (1992), "Interlaminar interface modeling for the prediction of laminate delamination", *Compos. Struct*., **22**, 235-242.

Barbero, E.J., Reddy, J.N. and Teply, J. (1990), "An accurate determination of stresses in thick laminates using a generalized plate theory", *Int. J. Numer. Meth. Eng.*, **29**, 1-14.

Barbero, E. and De Vivo, L. (2001), "A constitutive model for elastic damage in fiber-reinforced PMC laminae", *Int. J. Damage Mech.*, **10**, 73-93.

Barbero, E. and Lonetti, P. (2002), "An inelastic damage model for fiber reinforced laminates", *J. Compos. Mater.,* **36**(8), 941-962.

Belytschko, T., Liu, W.K. and Moran, B. (2000), *Nonlinear Finite Elements for Continua and Structures*, John Wiley and Sons Ltd., New York.

Chaboche, J.L. (1988a), "Continuum damage mechanics. Part I : General concepts", *J. Appl. Mech*., **55**, 59-64.

Chaboche, J.L. (1988b), "Continuum damage mechanics. Part II: Damage growth, crack initiation and crack growth", *J. Appl. Mech.,* **55**, 65-72.

Cordebois, J.L. and Sirodoff, F. (1979), "Damage induced elastic anisotropy", Colloque Euromech 115, Villard de Lans, France.

Herakovich, C.T. (1998), *Mechanics of Fibrous Composites*, John Wiley, New York.

Kachanov, L.M. (1958), "On the creep fracture time", *Zzu. Akad. Nauk. USSR Otd. Tekh*., **8**, 26-31 (in Russian).

Krajcinovic, D. (1983), "Constitutive equations for damaging materials", *J. Appl. Mech.,* **50**, 355-360.

Krajcinovic, D. (1984), "Continuum damage mechanics", *Appl. Me & Rev*., **37**(l), l-6.

Ladeveze, P., Allix, O. and Daudeville, L. (1990), "Mesomodeling of damae for laminate composites: Application to delamination", In: Inelastic Deformation of Composite Materials, et G,J, Dvorak, 607-622.

Ladeveze, P., Allix, O., Deu, J.F. and Leveque, D. (2000), "A mesomodel for localisation and damage computation in laminates", *Comput. Meth. Appl. Mech. Eng*., **183**, 105-122.

Ladeveze, P. and Le Dantec, E. (1992), "Damage modeling of the elementary ply for laminated composites", *Compos. Sci. Technol*., **43**(3), 257-267.

Lemaitre, J. (1985), "A continuous damage mechanics model for ductile fracture", *J. Eng. Mater. Technol.,* **107**, 83-89.

Lemaitre, J. (1986), "Local approach of fracture", *Eng. Fract. Mech*., **25**(5/6), 523-537.

Lonetti, P., Zinno, R., Greco, F. and Barbero, E. (2003), "Interlaminar damage model for polymer matrix composites", *J. Compos. Mater*., **37**(16), 1485-1504.

Talreja, R. (1985), "A continuum mechanics characterization of damage in composite materials", *Proc. R. Soc.* **A399**, 195-216.

Voyiadjis, G.Z. and Dorgan, R.J. (2007), "Framework using functional forms of hardening internal state variables in modeling elasto-plastic-damage behavior", *Int. J. Plasticity* (in Press).

Voyiadjis, G.Z. and Kattan, P.I. (1993), "Damage of fiber-reinforced composite materials with micromechanical characterization", *Int. J. Solids Struct.,* **30**(20), 2757-2778.

Voyiadjis, G.Z. and Deliktas, B. (2000), "A coupled anisotropic damage model for the inelastic response of composite materials", *Comput. Meth. Appl. Mech. Eng*., **183**, 159-199.

Voyiadjis, G.Z. and Kattan P.I. (1999), "Advances in damage mechanics: metals and metal matrix composites", Elsevier, Amsterdam.

Voyiadjis, G.Z. and Kattan, P.I. (1993), "Damage of fiber reinforced composite materials with micromechanical characterization", *Int. J. Solids Struct*., **30**, 2757-2778.

Voyiadjis, G.Z. and Park, T. (1999), "Kinematics description of damage for finite strain plasticity", *J. Eng. Sci.,* **37**, 803-830.